Available online at www.sciencedirect.com

ScienceDirect

Ceramics International 40 (2014) 4327–4332

CERAMICS INTERNATIONAL

www.elsevier.com/locate/ceramint

Optical properties of group-I-doped ZnO nanowires

Abdolhossein Sa´aedi[a], Ramin Yousefi[b,*], Farid Jamali-Sheini[c], Mohsen Cheraghizade[a],
A. Khorsand Zak[d], Nay Ming Huang[e]

[a]*Department of Electrical Engineering, Bushehr Branch, Islamic Azad University (I.A.U), Bushehr, Iran*
[b]*Depertment of Physics, Masjed-Soleiman Branch, Islamic Azad University (I.A.U), Masjed-Soleiman, Iran*
[c]*Department of Physics, Ahwaz Branch, Islamic Azad University, Ahwaz, Iran*
[d]*Nanotechnology Laboratory, Esfarayen University, North Khorasan, Iran*
[e]*Low Dimensional Materials Research Center, Department of Physics, Faculty of Science, University of Malaya, 50603 Kuala Lumpur, Malaysia*

Received 13 August 2013; received in revised form 21 August 2013; accepted 22 August 2013
Available online 30 August 2013

Abstract

Undoped and group-I elements doped ZnO nanowires were synthesized using a thermal evaporation method. Field emission scanning electron microscopy (FESEM) results showed that, the undoped ZnO nanowires were ultra-long with uniform diameters. On the other hand, the length of the doped ZnO nanowires was in the range of some hundred of nanometers. X-ray diffraction (XRD) patterns clearly indicated hexagonal structures for all of the products. X-ray photoelectron spectroscopy (XPS) studies confirmed the oxidation states of Li, Na, K, in the ZnO lattice. An asymmetric O 1s peak indicated the presence of oxygen in an oxide layer. The effect of doping on the optical band-gap and crystalline quality was also investigated using photoluminescence (PL), UV–vis, and Raman spectrometers. The Raman spectra of the products indicated a strong E_2 (high) peak. The PL spectra exhibited a strong peak in the ultraviolet (UV) region of the electromagnetic spectrum for all of the ZnO nanowires. The UV peak of the doped ZnO nanowires was red-shifted compared to the undoped ZnO nanowires. In addition, the UV–vis spectra of the samples showed similar results compared to the PL results.

Keywords: A. Films; C. Optical properties; D. ZnO

1. Introduction

Zinc oxide (ZnO) is an n-type metal oxide semiconductor with a wide band-gap (3.36 eV) and large exciton binding energy (60 meV) at room temperature. These characteristics make this material interesting for many applications such as solar cells [1], field emission materials [2], nano-electronic devices [3], gas sensor [4], and photocatalyst properties [5]. The key factors affecting these applications are the shape, size, impurities, doping, structures, and phases. For this reason, many researchers in recent years have focused on the synthesis of doped and undoped nanocrystalline materials such as ZnO. In addition to ours, many other groups have also reported the synthesis of doped ZnO nanostructures with various morphologies using different methods [6–9]. However, the key challenge that needs to be overcome for the realization of most ZnO based applications is the fabrication of p-type material. p-type ZnO may be achieved by the substitution of group-I elements on the Zn-site [10–12] and group-V elements on the O-site [13–15], respectively. Although many attempts has been made recently over the material conductivity type is still to be obtained and hence a comprehensive investigation of the fundamental properties of acceptors in ZnO is needed. From literature survey it is found that, the selected element from group-I elements showed better properties as dopants materials than group-V elements in terms of the shallowness of the acceptor level [16]. Therefore, the study of different effects of group-I as dopants on structural and optical properties of ZnO nanostructures can lead to obtain p-type ZnO nanostructures.

Several groups have tried to synthesize p-type ZnO nanostructures by employing group-I elements as acceptors. Recently, p-type Li-doped ZnO nanowires have been grown by our group, which were grown by a thermal evaporation method. It was observed that not only lithium could play as an acceptor in ZnO structures but also could improve the optical properties of the

---

[*] Corresponding author. Tel.: +98 916 6224993; fax: +98 681 3330093.
E-mail address: Yousefi.ramin@gmail.com (R. Yousefi).

0272-8842/$ - see front matter
http://dx.doi.org/10.1016/j.ceramint.2013.08.100

ZnO nanowires [3]. Jayanthi and co-workers compared the effects of Li and Na on the morphology of ZnO nanocrystals. They found that lattice parameters and the bond length of the Li- and Na-doped ZnO nanocrystals were altered due to different ionic radii of Li^+ and Na^+ [17]. In addition, Lee and Chang investigated possible p-type doping with the group-I elements in ZnO. They obtained that, Li and Na are better acceptor dopants with shallower acceptor levels than N, while they are mostly self-compensated by Li and Na interstitials, respectively. They also found that a co-doping with H impurities and a subsequent annealing process greatly enhance the electrical activity of group-I dopants [18]. Xiao et al. doped ZnO thin film with Li using pulsed laser deposition (PLD). They concluded that Li-doped ZnO thin film not only provided good p-type behavior but also showed high transmittance in the visible region [19]. In addition, a Li–N dual-acceptor doping method has been developed by Lu and co-workers to prepare p-type ZnO thin films using PLD [20]. They observed much lower resistivity for Li–N co-doped ZnO thin film than that of Li or N monodoped ZnO films. Therefore, a comparative study of different effects of group-I elements on morphology and optical properties of ZnO nanostructures can lead to better understanding of the behavior of these materials as acceptors in ZnO structure. Such knowledge can enhance development of optoelectronic devices in the future.

In the present work, a thermal evaporation route was used to grow undoped, Li-, Na, and K-doped ZnO nanowires. The effects of these elements from the group-I elements on morphology and optical properties of the ZnO nanowires were investigated.

2. Experimental sections

The growth of undoped and group-I-doped ZnO nanowires was performed in a horizontal tube furnace. First, Si (1 0 0) substrates were ultrasonically cleaned using ethanol and deionized water. They were then lightly etched with an HF (43%) and deionized water mixture (1:10) for about 10 min to remove the native oxide layer. A mixture of zinc oxide powder (99.99%), XOH powder (X=Li, Na, and K), and commercial graphite powder in a 10:1:10 weight ratio was used as the precursor material to grow the doped ZnO nanowires. The precursor material was placed at the closed end of a small quartz tube and a Si (1 0 0) substrate was placed downstream of the precursor material. The small tube was then inserted into the vacuum chamber so that the closed end was at the center of the furnace. The source material was heated up to 950 °C and the temperature of the substrate was maintained at 600 °C during growth. High purity N_2 gas was fed at about 200 sccm into the furnace at one end, while the other end was connected to a rotary pump. The growth process was allowed to proceed for 1 h. A vacuum of 50 Torr was maintained inside the tube furnace during the deposition of the nanostructures. According to these conditions, three sets of the group-I-doped ZnO nanowires were grown. In addition, the undoped ZnO nanowires were grown under the same conditions.

The morphology and crystal structure of the products were investigated using field emission scanning electron microscopy (FESEM, Hitachi S4160) and an x-ray diffraction (XRD, Phillips PW3040/60), respectively. Elemental analyses of the products were undertaken using x-ray photoelectron spectroscopy (XPS, VG-Microtech ESCA-2000). The XPS spectra were recorded using Mg-Kα radiation (1256.6 eV). Room temperature photoluminescence (Perklin Elmer LS55), UV–vis (Cary 500 UV–Vis–Nir), and Raman (Almega Thermo Nicolet Dispersive Raman Spectrometer) spectrometers were employed to study the optical properties and crystallinity of the ZnO nanowires. A xenon arc lamp as the light source was used for the PL and an Nd:YLF laser with a wavelength of 532 nm were used for the Raman measurements.

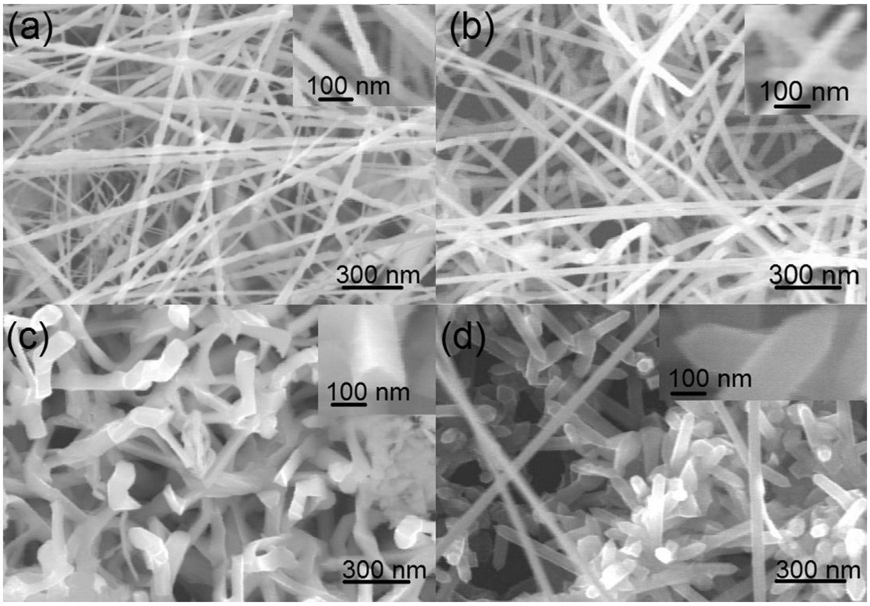

Fig. 1. FESEM images of (a) undoped, (b) Li-doped, (c) Na-doped, and (d) K-doped ZnO nanowires. The insets show end of the nanowires.

3. Results and discussion

Fig. 1(a)–(d) show the FESEM images of undoped and group-I-doped ZnO nanowires. As can be observed in this FESEM image, the undoped ZnO nanowires were randomly grown on the Si substrate, with a uniform diameter of ~50 nm and length of several hundred micrometers (Fig. 1(a)). Fig. 1(b) shows an FESEM image of the Li-doped ZnO nanowires. It can be seen in this image, the Li-doped ZnO nanowires were also randomly grown on the Si substrate, with similar diameter (~55 nm) in comparison to the undoped ZnO nanowires. Fig. 1(c) shows an FESEM image of the Na-doped ZnO nanorods with an average diameter of ~75 nm and length of several hundred nanometers. Fig. 1(d) reveals an FESEM image of the K-doped ZnO nanowires with an average diameter of ~110 nm with non-uniform length. In addition, the insets of these figures show that, the end of the nanowires shape is different.

Fig. 2 shows the XRD patterns of the undoped and group-I-doped ZnO nanowires. The XRD patterns agree with the standard card for bulk ZnO with a hexagonal structure (JCPDS No. 800075). No peaks from Zn, Li_2O, Na_2O, K_2O or other impurities are observed.

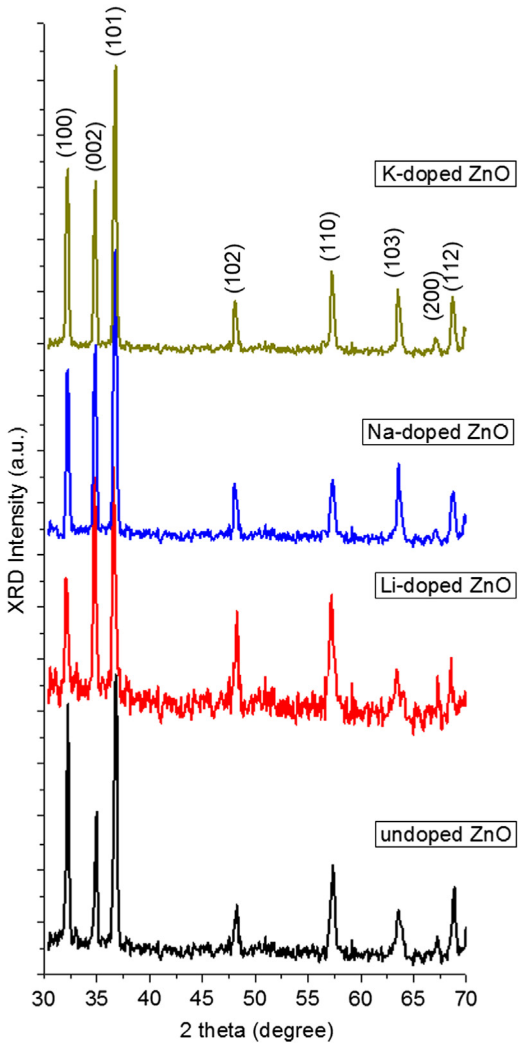

Fig. 2. XRD patterns of the undoped and group-I-doped ZnO nanowires.

The XPS analysis was used for further evaluation of their purity and the composition of the film′s surface within a few nanometers and is depicted in Fig. 3. These spectra show an overall scan, indicative of group-I seepage in ZnO structures. In Fig. 3(a) the photoemission peak located at 55.8 eV for Li-1s, at 1071.8 eV for Na-1s in Fig. 3(b), and at 291 eV for K-2p in Fig. 3(c) shows the seepaging of group-I impurities in the atomic structure of ZnO. In all cases, the spin orbit splitting of 23 eV for Zn-$2p_{3/2}$ and Zn-$2p_{1/2}$ confirming that the Zn atoms are in a completely oxidized state [21]. Also photoemission peak for Zn and O is obvious in Fig. 3. The peak exhibited at 532.1 eV to 532.4 eV is attributed to the oxidized metal ions in the films, namely O–Zn in the ZnO lattice.

Raman spectroscopy is an effective technique for estimating the crystallinity of materials. According to the group theory, single crystalline ZnO belongs to the C_{6v}^{4} space group, with two formula units per primitive cell and eight sets of optical phonon modes at the Γ point of the Brillouin zone, classified as $A_1+E_1+2E_2$ modes (Raman active), $2B_1$ modes (Raman silent) and A_1+E_1 modes (infrared active). The E_1 and A_1 modes are two polar modes and are split into the transverse optical (TO), and longitudinal optical (LO) branches. The Raman spectra of the undoped and group-I-doped ZnO nanowires are presented in Fig. 4. As shown in Fig. 4, the Raman spectra show a sharp, strong, and dominant peak at 438 cm^{-1} for the nanowires, corresponding to the E_2 (high) mode of the Raman active mode, a characteristic peak for the wurtzite hexagonal phase of ZnO. The peak at 579 cm^{-1} belongs to E_1(LO) is associated with impurities and the formation of defects such as oxygen vacancies [22]. However, this result indicates that the Li-doped ZnO nanowires have lower oxygen vacancies than the Na-, K-doped, and undoped ZnO nanowires.

Photoluminescence (PL) study is also a powerful method for investigating the effects of impurity doping on the optical properties of semiconductor nanostructures with direct band gap, because doped nanostructures are expected to have different optical properties compare to undoped nanostructures. Fig. 5 shows the room temperature PL spectra of the undoped and group-I-doped ZnO nanowires. The PL spectra of the undoped and doped ZnO nanowires show a strong peak in the ultraviolet (UV) region at 381–388 nm, and a green emission (deep-level emission (DLE)) peaks in the visible region at ≈490–540 nm. However, the UV/DLE ratio of the Li-doped ZnO nanowires, which is one of the main factors that is usually used for comparing the optical properties of samples, is bigger than the UV/DLE ratio of the Na-, K-doped, and undoped ZnO nanowires. Therefore, the Li-doped ZnO nanowires have a better relative crystalline quality. This result indicates that the Li-doped ZnO nanowires have higher optical quality than Na-, K-doped, and undoped ZnO nanowires. This result is in good agreement with our previous results [10]. In addition, these results are in good agreement with those obtained from the Raman results. Seemingly, the PL results indicate that Li from the group-I elements can reduce oxygen vacancies in ZnO lattice. The Raman results obtained from Fig. 4 show that, the Li-doped ZnO nanowires have significantly smaller deffect than the other ZnO nanowires. It is known that defects can decrease the crystalline and optical qualities of a sample [23]. However, the main reason to obtain these results could be ionic radii difference. Since Li (0.76 Å) has similar ionic radius with Zn (0.74 Å) in comparison to Na (1.02 Å) and K (1.38 Å) that have bigger ionic radii than Zn. The incorporation of the ghost element with the big difference of ionic radius into the host lattice will introduce lattice distortion. This effect influences the energy band structure of the ZnO nanowires doped with sodium and potassium, and as a result, new defects such as oxygen vacancies can be introduced by the new band structure deformation. Compared with the undoped ZnO nanowires, the PL spectra of the doped ZnO nanowires show an obvious red-shift in the UV emission (Fig. 5(b)). This red-shift in the UV emission could be a result to obtain p-type ZnO nanowires. A widening of the band-gap is usually observed for ZnO doped with donors; while p-type ZnO has shown band-gap reduction if doped with acceptors. In fact, the UV peak of the PL spectra of the ZnO nanostructures, which have been doped by donor materials, exhibited a blue-shift in comparison to that observed for the undoped ZnO nanostructures [24–26].

For better understanding the effects of the group-I elements on the optical properties of the ZnO nanowires, the nanowires have been characterized by UV–vis spectroscopy. Fig. 6 shows the UV–vis absorbance spectra of the undoped and doped ZnO nanowires. The absorbance spectrum intensity is increased and emission band has a red-shift after the group-I doping. Moreover, the direct band-gap energies can be estimated from a plot of $(\alpha \times h\nu)^2$ versus the photo energy ($h\nu$) according to the Kubelka–Munk model [27], where α is the absorptance coefficient, h is plank constant, and ν is frequency. In addition, the direct band gap can be estimated from the maximum of the first derivative of the absorbance plot versus energy also from the intersection of the second derivative with energy axle [27]. Fig. 6(b) shows the second derivative of the absorbance

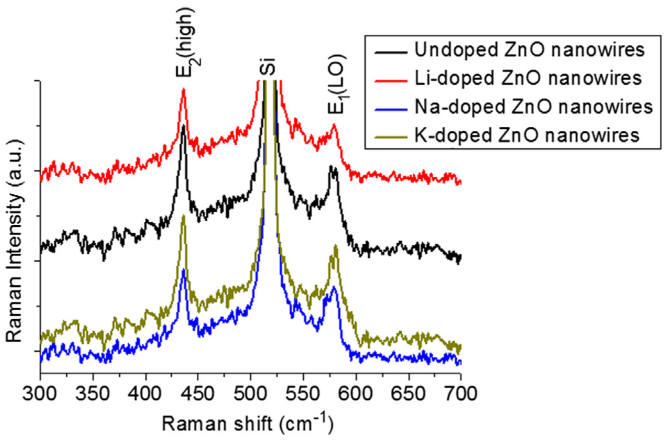

Fig. 4. Raman spectra of the undoped and group-I-doped ZnO nanowires.

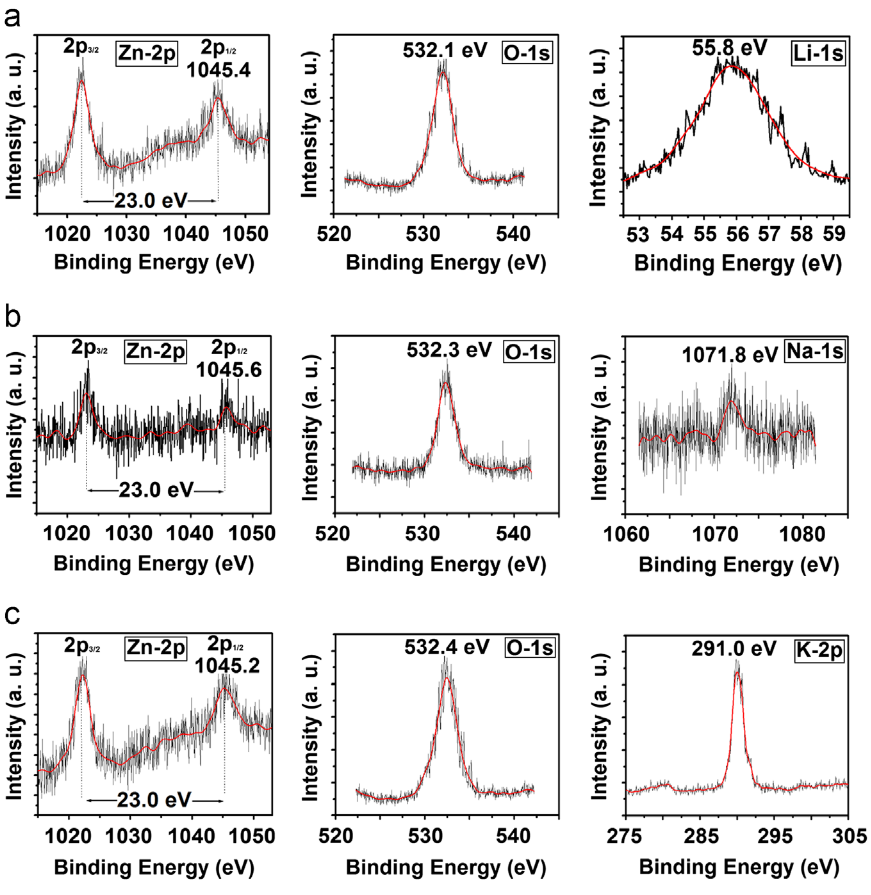

Fig. 3. XPS spectra of (a) Li-doped, (b) Na-doped, and (c) K-doped ZnO nanowires.

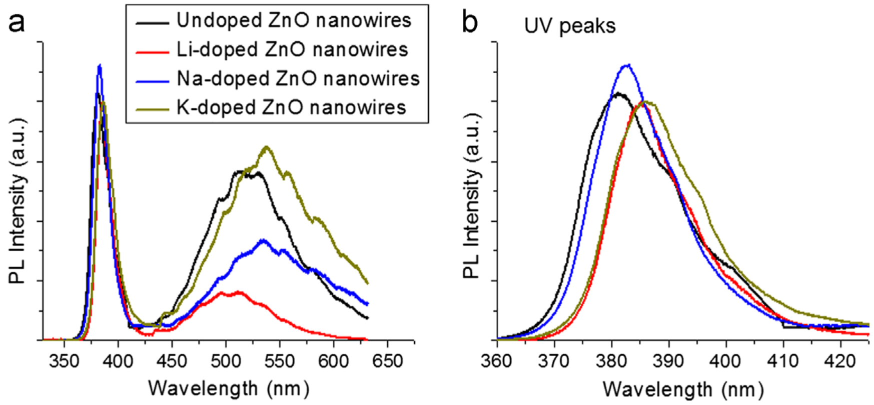

Fig. 5. (a) PL spectra of the undoped and group-I-doped ZnO nanowires. (b) UV peaks of the nanowires.

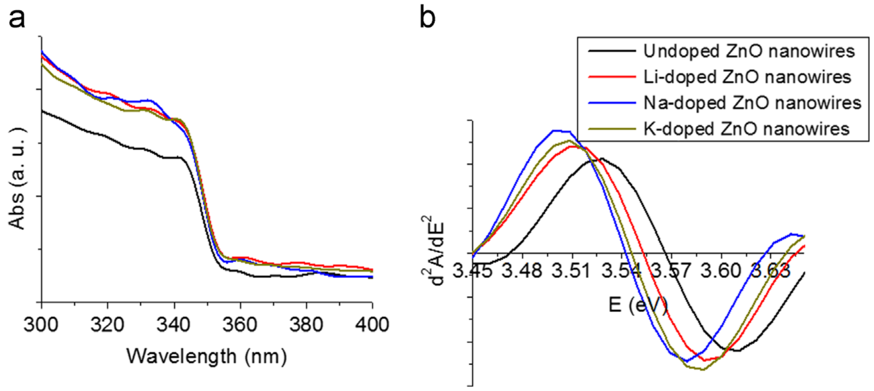

Fig. 6. (a) Absrobance spectra of the undoped and group-I-doped ZnO nanowires. (b) The band gap of the ZnO nanowires estimated from second derivative and energy excel intersect.

coefficient for the undoped and group-I-doped ZnO nanowires. This method also shows decreasing of optical band gap energy of the group-I-doped ZnO nanowires in comparison to the undoped ZnO nanowires.

4. Conclusion

The thermal evaporation method was used to grow undoped, Li-, Na-, and K-doped ZnO nanowires. The FESEM results showed that, the group-I elements as dopants not only changed the size of the nanowires but also they changed the face of the nanowires. The XRD patterns indicated a hexagonal phase for all of the nanowires. The XPS spectra revealed that, indicative of group-I seepage in ZnO structures. In addition, the XPS spectrum of Zn 2p showed that the split value of binding energy could be a characteristic value of ZnO. Optical characterization revealed that, the band gap energy of the ZnO nanowires reduced due to group-I elements as dopants.

Acknowledgement

R. Yousefi and F. Jamali Sheini gratefully acknowledge the Islamic Azad University (I.A.U), Masjed-Soleiman and Ahwaz Branches, respectively, for their financial support of this research work. In addition, N. M. Huang acknowledges obtaining a High Impact Research Grant from the Ministry of Higher Education of Malaysia (UM.C/P/HIR/MOHE/SC/21).

References

[1] A. Qurashi, M.F Hossain, M. Faiz, N. Tabet, M.W Alam, N.K Reddy, Fabrication of well-aligned and dumbbell-shaped hexagonal ZnO nanorod arrays and their dye sensitized solar cell applications, Journal of Alloys and Compounds 503 (2010) L40–L43.

[2] F. Jamali-Sheini, D.S. Jag, Mahendra A. More, Field emission studies on electrochemically synthesized ZnO nanowires, Ultramicroscopy 109 (2009) 418–422.

[3] A. Sáaedi, R. Yousefi, F. Jamali-Sheini, M. Cheraghizade, A. Khorsand Zak, N.M. Huang, Optical and electrical properties of p-type Li-doped ZnO nanowires, Superlattices and Microstructures 61 (2013) 91–96.

[4] A. Qurashi, M. Faiz, N. Tabet, M. Waqas Alam, Low temperature synthesis of hexagonal ZnO nanorods and their hydrogen sensing properties, Superlattices and Microstructures 50 (2011) 173–180.

[5] S. Khameneh Asl, S.K. Sadrnezhaad, M. Kianpour Rad, The seeding effect on the microstructure and photocatalytic properties of ZnO nano powders, Materials Letters 64 (2010) 1935–1938.

[6] R. Yousefi, A. Khorsand Zak, F. Jamali-Sheini, Growth, X-ray peak broadening studies, and optical properties of Mg-doped ZnO nanoparticles, Materials Science in Semiconductor Processing 16 (2013) 771–777.

[7] M.K. Gupta, N. Sinha, B.K. Singh, B. Kumar, Synthesis of K-doped p-type ZnO nanorods along (100) for ferroelectric and dielectric applications, Materials Letters 64 (2010) 1825–1828.

[8] A.A. Ibrahima, G.N. Darb, S.A. Zaidia, A. Umara, M. Abakerb, H. Bouzidb, S. Baskoutasd, Growth and properties of Ag-doped ZnO

nanoflowers for highly sensitive phenyl hydrazine chemical sensor application, Talanta 93 (2012) 257–263.

[9] R. Yousefi, F. Jamali-Sheini, A. Sa′aedi, A. Khorsand Zak, M. Cheraghizade, S. Pilban-Jahromi, N.M. Huang, Influence of lead concentration on morphology and optical properties of Pb-doped ZnO nanowires, Ceramics International http://dx.doi.org/10.1016/j.ceramint.2013.05.008.

[10] R. Yousefi, A. Khorsand Zak, F. Jamali-Sheini, The effect of group-I elements on the structural and optical properties of ZnO nanoparticles, Ceramics International 39 (2013) 1371–1377.

[11] W. Liu, F. Xiu, K. Sun, Y.H. Xie, K.L. Wang, Y. Wang, J. Zou, Z. Yang, J. Liu, Na-doped p-type ZnO Microwires, Journal of the American Chemical Society 132 (2010) 2498–2499.

[12] X.P. Yang, J.G. Lu, H.H. Zhang, Y. Chen, B.T. Kan, J. Zhang, J. Huang, B. Lu, Y.Z. Zhang, Z.Z. Ye, Preparation and XRD analyses of Na-doped ZnO nanorod arrays based on experiment and theory, Chemical Physics Letters 528 (2012) 16–20.

[13] L. Li, C.X. Shan, B.H. Li, B. Yao, J.Y. Zhang, D.X. Zhao, Z.Z. Zhang, D.Z. Shen, X.W. Fan, Y.M. Lu, The compensation source in nitrogen doped ZnO, Journal of Physics D: Applied Physics 41 (2008) 245402-1-4.

[14] B. Yao, Y.P. Xie, C.X. Cong, H.J. Zhao, Y.R. Sui, T. Yang, Q. He, Mechanism of p-type conductivity for phosphorus-doped ZnO thin film, Journal of Physics D: Applied Physics 42 (2009)015407-1-4 42 (2009).

[15] D. Yu, L. Hu, S. Qiao, H. Zhang, S.E.A. Len, L.K. Len, Q. Fu, X. Chen, K. Sun, Photoluminescence study of novel phosphorus-doped ZnO nanotetrapods synthesized by chemical vapor deposition, Journal of Physics D: Applied Physics 42 (2009) 055110-1-6.

[16] Y.J. Zeng, Z.Z. Ye, J.G. Lu, W.Z. Xu, L.P. Zhu, B.H. Zhao, S. Limpijumnong, Identification of acceptor states in Li-doped p-type ZnO thin films, Applied Physics Letters 89 (2006) 042106-1-3.

[17] K. Jayanthi, S. Chawla, K.N. Sood, M. Chhibara, S. Singh, Dopant induced morphology changes in ZnO nanocrystals, Applied Surface Science 255 (2009) 5869–5875.

[18] E.C. Lee, K.J. Chang, Possible p-type doping with group-I elements in ZnO, Physical Review B: Condensed Matter 70 (2004) 115210-1-4.

[19] B. Xiao, Z. Ye, Y. Zhang, Y. Zeng, L. Zhu, B. Zhao, Fabrication of p-type Li-doped ZnO films by pulsed laser deposition, Applied Surface Science 253 (2006) 895–897.

[20] J.G. Lu, Y.Z. Zhang, Z.Z. Ye, L.P. Zhu, L. Wang, B.H. Zhao, Q.L. Liang, Low-resistivity, stable p-type ZnO thin films realized using a Li–N dual-acceptor doping method, Applied Physics Letters 88 (2006) 222114-1-3.

[21] F. Jamali-Sheini, Chemical solution deposition of ZnO nanostructure films: Morphology and substrate angle dependency, Ceramics International 38 (2012) 3649–3657.

[22] R. Yousefi, B. Kamaluddin, Effect of S and Sn doping to the optical properties of ZnO nanobelts, Applied Surface Science 255 (2009) 9376–9380.

[23] R. Yousefi, F. Jamali-Sheini, A. Khorsand Zak, A comparative study of the properties of ZnO nano/microstructures grown using two types of thermal evaporation set-up conditions, Chemical Vapor Depositio 18 (2012) 215–220.

[24] R. Yousefi, F. Jamali-Sheini, Effect of chlorine ion concentration on morphology and optical properties of Cl-doped ZnO nanostructures, Ceramics International 38 (2012) 5821–5825.

[25] R. Yousefi, F. Jamali-Sheini, A. Khorsand Zak, M.R. Mahmoudian, Effect of indium concentration on morphology and optical properties of In-doped ZnO nanostructures, Ceramics International 38 (2012) 6295–6301.

[26] R. Yousefi, M.R. Muhamad, Effects of gold catalysts and thermal evaporation method modifications on the growth process of $Zn_{1-x}Mg_xO$ nanowires, Journal of Solid State Chemistry 183 (2010) 1733–1739.

[27] A.Khorsand Zak, W.H.Abd. Majid, M.R. Mahmoudian, M. Darroudi, R. Yousefi, Starch-stabilized synthesis of ZnO nanopowders at low temperature and optical properties study, Advanced Powder Technology 24 (2013) 618–624.